BOREAS An international journal of Quaternary research

Variations in tephra stratigraphy created by small-scale surface features in sub-polar landscapes

POLLY I. J. THOMPSON, ANDREW J. DUGMORE, ANTHONY J. NEWTON, RICHARD T. STREETER AND NICK A. CUTLER

BOREAS

Thompson, P. I. J., Dugmore, A. J., Newton, A. J., Streeter, R. T. & Cutler, N. A.: Variations in tephra stratigraphy created by small-scale surface features in sub-polar landscapes. *Boreas*. https://doi.org/10.1111/bor.12557. ISSN 0300-9483.

We explore the effect small-scale surface features have on influencing the morphology and grain-size distribution (GSD) of tephra layers within the Quaternary stratigraphy of sub-polar landscapes. Icelandic thúfur, small cryogenic earth mounds, are used to assess how and why the morphology and GSD of tephra layers vary over such formations. Through measurement of tephra layer thickness and GSD, Hekla 1947 and Grímsvötn 2011 tephra layers are analysed. Results indicate that such microtopographic features do indeed alter the form of tephra deposits and therefore the tephra layer that is preserved in the stratigraphy. Tephra thickness is significantly greater in hollows than on the thúfur crests. There is greater variation in tephra thickness measurements from thúfur in comparison to control measurements from a surface where thúfur are absent. Thúfur crests contain larger grain sizes than hollows, for both H1947 and G2011 tephras; however this was only statistically significant for the G2011 tephra. Such morphological patterns are thought to arise from an interplay of tephra characteristics, altered topography from the thúfur formations and earth surface processes operating at the sites. This study provides insight into the potential of tephra layer morphology and internal structures as indicators of Quaternary landforms and processes. Additionally, it provides important context for the appropriate sampling of tephra layers to infer volcanological processes, as the characteristics of preserved layers do not necessarily reflect those of the original fall-out.

Polly Thompson (polly.thompson@ed.ac.uk), Andrew J. Dugmore and Anthony J. Newton, Institute of Geography, School of GeoSciences, University of Edinburgh, Edinburgh EH8 9XP, UK; Richard T. Streeter, School of Geography & Sustainable Development, University of St Andrews, St Andrews KY16 9AL, UK; Nick A. Cutler, School of Geography, Politics and Sociology, Newcastle University, Newcastle upon Tyne NE1 7RU, UK; *received 2nd June 2021, accepted 13th August 2021.*

Tephra can undergo numerous alterations post deposition before being preserved as an enduring stratigraphical layer (Dugmore *et al*. 2020). The effect small-scale surface features have on the preservation of tephra has not yet been explored. Earth hummocks, known as thúfur (þúfur) in Iceland are small, dome-shaped cryogenic earth mounds characteristic of sub-polar locations (Fig. 1), and are used as exemplars in this pilot study, as similar topographically controlled processes will operate in different landscapes. Thúfur are features of permafrost and climatic state, providing an indication of environmental conditions (Grab 2005; Pintaldi *et al*. 2016). Thúfur formations result from freeze–thaw activity in high-latitude, or high-altitude, areas and are usually covered by vegetation (Van Vliet-Lanoë & Seppälä 2002; Grab 2005; Pintaldi *et al*. 2016; Fig. 1). Thúfur are a common cryogenic landform and are found globally across high-latitude areas such as Iceland, Greenland, Russia and Canada, as well as in upland areas at lower latitudes that contain enough soil for them to form, such as Dartmoor in southwestern England (Grab 2005). Such small-scale (width, height and/or length ~20–250 cm) topographic features are important landforms for inferring current and past earth surface processes and land management.

It is important to understand how small-scale surface features alter tephra layers because in addition to forming chronological markers, they are also used to infer the parameters of past eruptions (Lowe 2011). Both approaches make assumptions about the tephra. For example, tephrochronology assumes that the eruption and deposition dates are simultaneous. Volcanogenic inference (using tephra deposits to infer eruption parameters such as volume) relies on the assumption that the tephra layer is representative of the material that was deposited at the time of the eruption (Bonadonna & Houghton 2005; Engwell *et al*. 2013; Cutler *et al*. 2018).

However, tephra deposits are rarely preserved in their original form and their transformation is often regarded as an unhelpful complication. Deposits can undergo a series of morphological alterations soon after deposition, such as compaction, reworking (by wind and/or water), bioturbation and frost action, which can individually or collectively alter what is preserved as an enduring tephra layer (Blong *et al*. 2017; Dugmore *et al*. 2020). Postdepositional alterations can make the interpretation of tephra layers (e.g. in traditional tephrochronology and volcanological reconstruction) much more challenging (Lowe 2011; Dugmore & Newton 2012). However, distorted tephra layers have the potential to record past surface features, climate and subsequent subsurface processes, such as solifluction and cryoturbation (Matheus *et al*. 2003; Sanborn *et al*. 2006; Streeter & Dugmore 2013). This provides an

DOI 10.1111/bor.12557

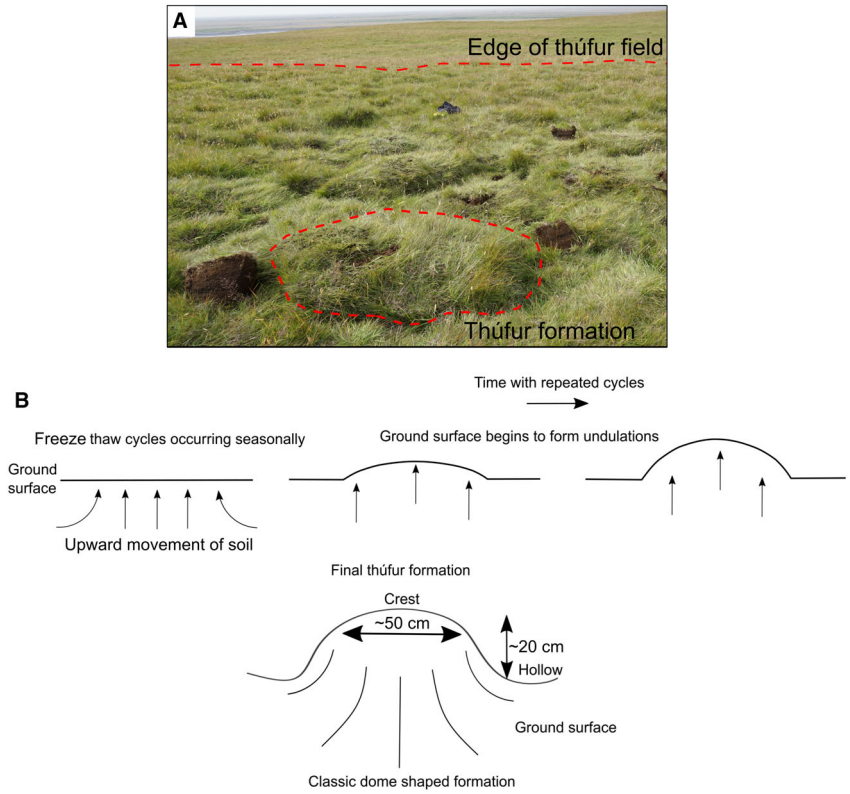

Fig. 1. A. Location photo of the thúfur field surveyed at Site B in south Iceland. B. A schematic diagram of how a thúfur forms by cryoturbation action and the resulting single thúfur formation with a relative relief and width of 20 and 50 cm, respectively, similar to those measured in this study.

opportunity to extract data on past environmental conditions. For example, undulating tephra layers that define closely spaced crests and hollows can signify the presence of thúfur on the surface. If we are to extract relevant proxy environmental data from the characteristics of tephra layers, we need to be able to distinguish between those features acquired by the deposit on the surface and those acquired once the deposit becomes a stratigraphical layer. This allows us to identify features that are properties of tephra fall or features reflecting surface conditions.

Assessment of tephra deposits across thúfur have indicated differences in the thicknesses of tephra on crests and in hollows, despite a uniform vegetation cover and thickness of the initial deposit. We therefore seek to determine how tephra preservation is influenced by microtopography, and what alterations in the thickness, layer morphology and grain-size distribution of tephra occur (Dugmore *et al*. 2018, 2020). Surface vegetation structures are known to affect the stabilization and preservation of tephra deposits, and at scales of 10s–100s of metres vegetation cover is more critical in determining preservation than slope or location on a slope of up to 35° (Cutler *et al*. 2016a, b; Dugmore *et al*. 2018). Examining thúfur formations will help to determine whether the presence of undulations on the surface overrides the vegetation present in terms of tephra preservation, and examines micro slope angles >35°.

Thus, this paper assesses whether tephra layers retain a signal of surface microtopography at the time of deposition and examines the transformation of the tephra during the period between its deposition and its burial. To understand these processes in greater detail, we designed a natural experiment studying two recent tephra layers that were deposited across thúfur formations to determine the impacts of such small-scale morphological features on tephra layer formation. The formation of subaerial tephra layers takes months to years and is difficult to observe directly. To allow for enough time to have passed, but ensure that surface conditions at the time of deposition were similar, our field survey in 2019 studied two Icelandic tephra layers 72 and 8 years after their respective eruptions. These tephra layers were formed by the eruption of Hekla in April 1947 and the eruption of Grímsvötn in May 2011. Our objectives are to measure the thickness and grain-size distribution of tephra layers deposited across areas of thúfur and our aim is to understand how small-scale surface features can create lasting morphological and sedimentological variations in the Quaternary tephrostratigraphical record. The terminology in this paper follows Dugmore *et al*. (2020), where the term tephra deposit is used to define

tephra that has accumulated on the surface, and tephra layer describes a visible horizon of tephra bounded by sediments on its top and bottom surfaces.

Study areas

We sampled tephra thickness and grain-size distribution (GSD) over crests and hollows of thúfur from the two tephra layers at sites in southern Iceland. These samples were then analysed to determine if there is a significant difference in tephra thickness, morphology and GSD between the crests and hollows of thúfur and therefore if these geomorphological features have an effect on tephra preservation. Surveys were conducted at three sites spanning two different locations within Iceland in June and August 2019, focusing on the Hekla 1947 (H1947) and Grímsvötn 2011 (G2011) tephra layers (Figs 2, 3). Iceland has numerous volcanoes, with an eruption occurring on average every 3–4 years (Thordarson & Larsen 2007). The frequent tephra production, coupled with silty loessial soils of contrasting grain sizes and colours that have high sediment accumulation rates (SeAR), create numerous, clearly identifiable well-separated, isochronous (age-equivalent) tephra layers. Sub-polar environmental conditions lead to extensive areas of thúfur formation, and this combination of factors makes Iceland an ideal location to investigate the impact of microtopographic variation on tephra layer preservation (Thorarinsson 1944; Arnalds 2005; Dugmore & Newton 2012; Streeter & Dugmore 2014).

We measured and sampled the H1947 tephra at two sites (A and B on Fig. 2) located in the area of Hamragarður in south Iceland, on the lower western slopes of Eyjafjallajökull (Table 1). The elevation of Site A was 241 m and of Site B was 90 m a.s.l. The closest weather station with historical records to Sites A and B is located in Vatnsskarðshólar (~40 km east). From 1949 to 2020, average yearly temperature ranged from 4 to 6.6 °C, with the average temperature in 1949 (2 years after the eruption and the earliest available year in the record) 4.9 °C. Average yearly precipitation varied from 882 to 2042 mm, with 1498 mm of precipitation in 1949 (Icelandic Meteorological Office 2021).

The H1947 eruption occurred in spring, beginning on 29th March and ending on 21st April. During the Plinian phase of the eruption (the first few hours) it is estimated that 180 million cubic metres of ash, pumice, bombs and scoria were erupted and dispersed in a southerly direction, covering over ~3000 km^2 in tephra (Thorarinsson 1956; Rea *et al*. 2012; Cutler *et al*. 2018). H1947 is a coarse-grained dark tephra, easily identifiable in the field from its stratigraphical position close to the surface (<0.5 m deep), range of pumice colours from grey/brown to black and the occurrence of small pieces of red scoria within the layer.

We measured and sampled the G2011 tephra layer at a third site (C, Fig. 3) at Kálfafell in southeast Iceland (Table 1). The elevation of Site C was 149 m a.s.l. The closest weather station to Site C with historical records is Kirkjubæjarklaustur (30 km southwest). From 1939 to 2012, average yearly temperature ranged from 3.2 to 6 °C, with the average temperature in 2012 (the year following the eruption) 5.3 °C. Average yearly precipitation varied from 1207 to 2442 mm, with 1990 mm of precipitation in 2012 (Icelandic Meteorological Office 2021). The G2011 tephra layer is fine–very fine grained with a uniform grey colour, although it is darker when wet. At Kálfafell, the G2011 layer was found a few centimetres below the surface.

The G2011 eruption occurred in late spring, beginning on 21st May and ending on 28th May 2011 (Liu *et al*. 2014). The interaction between glacial meltwater and magma initiated a phreatomagmatic style eruption. The eruption was short-lived, but intense, with a Volcanic Explosivity Index Magnitude of 4 (Guðmundsson *et al*. 2012; Cabré *et al*. 2016). The eruption generated a total (bulk) volume of tephra of 0.7 km^3 (Guðmundsson *et al*. 2012) and had a plume height of <20 km (Horwell *et al*. 2013). The axis of tephra dispersal during the 2011 eruption was in a (generally) southerly direction from the volcano (Dugmore *et al*. 2018).

We assumed that in terms of its influence on tephra deposition, the vegetation cover in 2019 was broadly the same as during the deposition of H1947 and G2011. Examining aerial photographs from 2 years before the eruption in 1947 confirms that the land cover was similar to today's (NCAP 2021). Site C where the G2011 tephra was sampled was also visited in 2012 and the vegetation in 2019 was comparable. These sites were chosen as they had numerous, well-developed thúfur. Sites A and B had higher plant diversity than Site C. As well as grass and moss, thyme (*Thymus vulgaris*), blueberry (*Vaccinium* sp.), crowberry (*Empetrum nigrum*) and patches of dwarf birch (*Betula nana*) were all present. Species cover at Site C in Kálfafell was limited to moss and grass species. The initial H1947 deposit thickness at Hamragarður was ~50 mm (Thorarinsson 1956). Approximately 10–20 mm of G2011 tephra was deposited at Kirkjubæjarklaustur (Stevenson *et al*. 2013), 30 km from Site C at Kálfafell. Thickness measurements collected by Cabré *et al*. (2016) from Skeiðarársandur (49 km from the volcanic vent and ~20 km from Kálfafell) ranged from 5 to 250 mm.

Material and methods

Field sampling

The ways in which small-scale topographic features affect tephra layer morphology and grain-size distribution (GSD) were assessed with a combination of field observations and laboratory experiments. We assessed differences in tephra preservation by taking paired measurements of tephra layer thickness from thúfur crests and adjacent hollows. Samples of tephra were

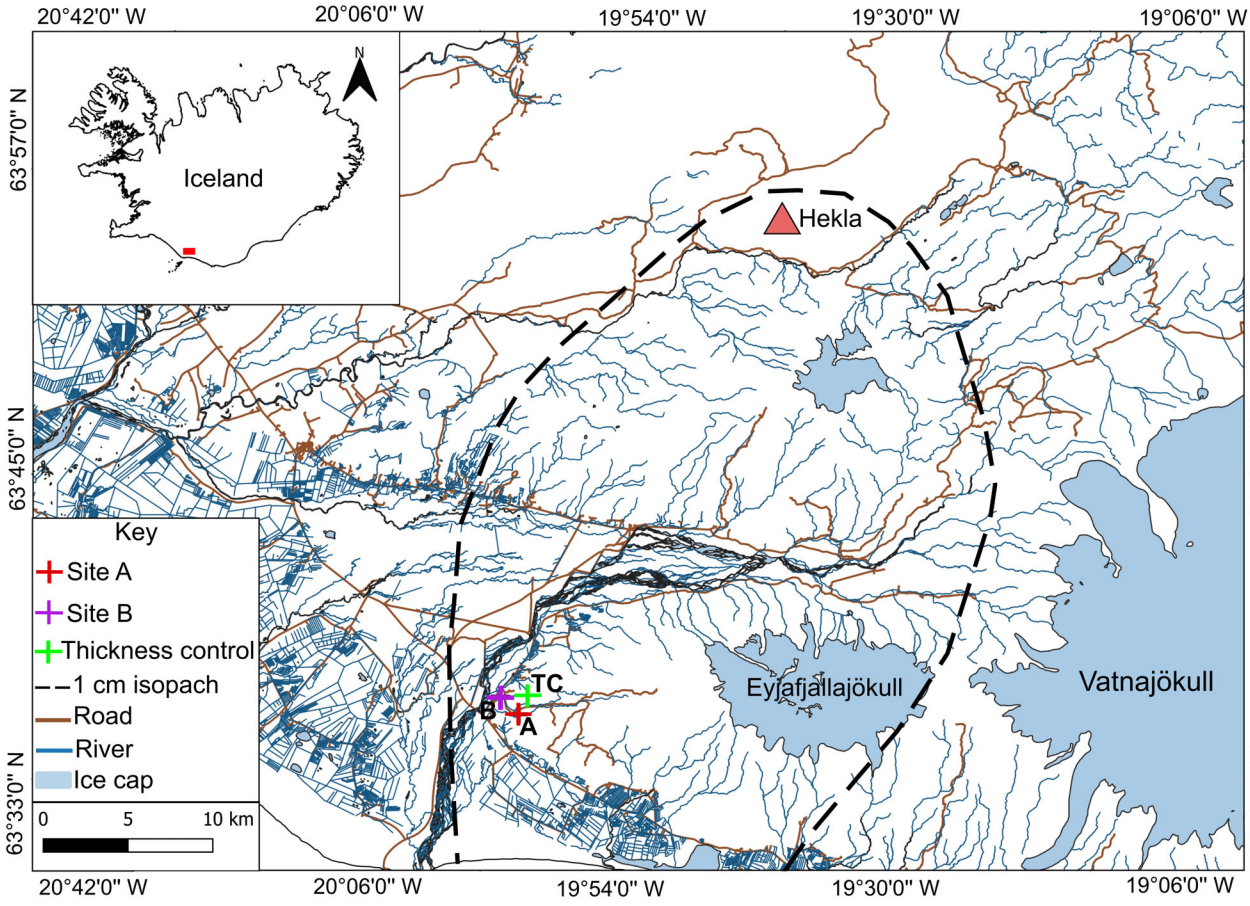

Fig. 2. Location of Sites A and B in Hamragarður where thickness measurements of the H1947 tephra were collected from 50 thúfur formations at Site A and measurements and tephra samples from 43 thúfur formations at Site B. Control sites are also marked, TC indicates the location of the thickness control transect. The location of the Hekla volcano that produced H1947 in relation to the sites is marked and the direction of the ash plume is indicated by the 1-cm isopach (adapted from Cutler *et al.* 2018).

collected from sampling locations within Sites B and C to measure differences in GSD between crests and hollows. Prior to data collection, a power analysis on pilot data was conducted to determine the optimum number of measurements required. The power analysis was based on 11 pairs of H1947 thickness measurements collected from thúfur crests and hollows (n = 22). In this data set, the mean tephra thickness was lower on the crests (11.3 mm) than in the hollows (18.5 mm), but the difference was not significant (paired t-test: t (10) = 1.624, p = 0.13). Power analysis was conducted using the function power.t.test in R (R Core Team 2019), with the following parameters: mean tephra thickness = 15 mm; standard deviation = 9 mm, effect size = 25% (4 mm) and power = 0.8. The results indicated that a minimum of 42 thúfur (n = 41.70) should be surveyed (paired measurements).

At each site, a suitable cluster of thúfur formations was identified by inspection. The size of the survey area reflected the density of earth hummocks, but in all cases was comparable in terms of vegetation, slope and elevation; Site A was 224 m^2, Site B was 100 m^2 and Site C was 56 m^2. Each cluster had well-developed thúfur, with a relative relief of at least ~20 cm and diameter ~50 cm. A small block of surface vegetation and the underlying soil 20×25×30 cm deep was then removed intact from each selected thúfur crest and the adjoining hollow to allow the tephra to be measured. Three representative measurements of the overlying soil thickness and the tephra layer thickness were taken from three sides of the excavated block at a resolution of ±1 mm. The measurements were taken directly from the middle of the block extracted from the crest and the hollow so that they were systematic and taken from the same place on each thúfur formation. Samples for GSD were also taken in this way. These measurements were averaged to give a mean soil thickness and tephra layer thickness for each thúfur crest and hollow. This process was repeated at each site for every thúfur sampling location surveyed within the cluster. The number of samples collected for grain-size analysis is summarized in Table 1. A sample of the entire layer was collected from

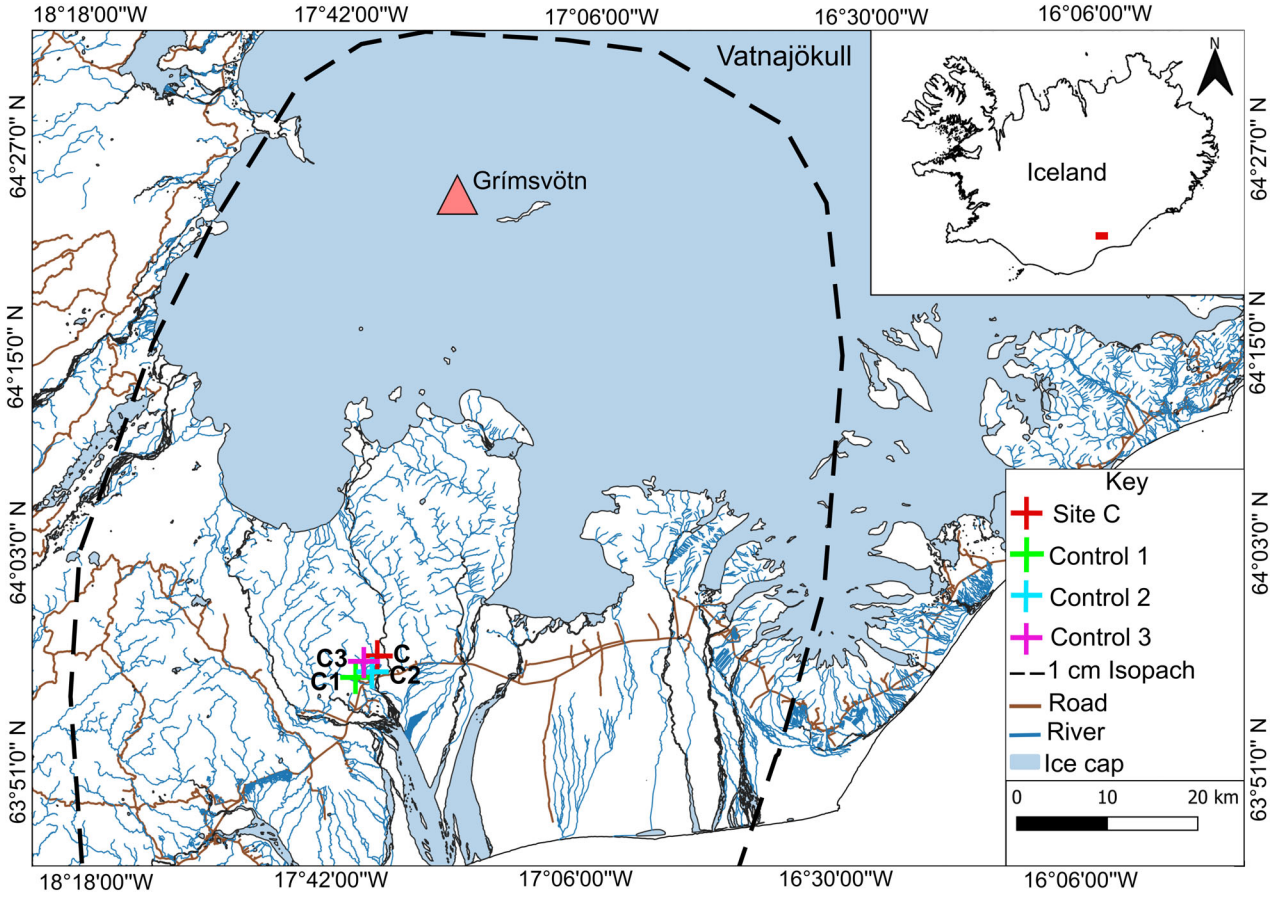

Fig. 3. Location of Site C in Kálfafell where thickness measurements and samples of the G2011 tephra were collected from 43 thúfur formations. The three thickness control sites are indicated by C1, C2 and C3. C1 also had grain-size control samples collected. The location of the Grímsvötn volcano that produced G2011 in relation to the sites is marked and the direction of the ash plume indicated by the 1-cm isopach (adapted from Thordarson & Höskuldsson 2014 and Dugmore *et al.* 2018).

every crest and hollow (where there was a tephra layer present) on each thúfur.

Control sets of measurements were collected to obtain tephra layer thickness from a site with no thúfur. The control site in Hamragarður was located <1 km from Sites A and B on a moss heath area with no notable gradient or undulations. The thickness of the H1947 tephra layer was measured every centimetre along a 4.8-m-long transect (Fig. 2). Three control sets of measurements from Kálfafell were also used (Fig. 3); Control 1 was collected in Blómsturvellier from a rofabard (an Icelandic erosion feature, see Arnalds 2000) with measurements obtained 5–15 m from the edge of the escarpment (100 measurements in total, measured every 5 cm). Controls 2 and 3 were both collected in Kálfafell and presented in Cutler *et al.* (2016a) as sites Kálfafell (moss, K_m) and Kálfafell (grass, K_g). Control 2 consisted of 200 measurements, collected every 12.5 cm and Control Site 3 consisted of 120 measurements, collected from 24 pits at 5-m intervals along a transect. Further details about the control data sets used are provided in Data S1.

Grain-size analysis

GSD of samples was measured by laser diffraction granulometry, using a Beckmann Coulter LS230 with a PIDS detector. Samples of tephra were prepared and the grain-size distribution analysed following the steps outlined in Data S2. H1947 is a coarse-grained tephra with lithic and pumice clasts; thus each sample was sieved so that clasts larger than 2000 μm were not processed through the grain-size analyser, as this is the maximum size fraction that can be measured. This coarser fraction was sieved using half phi sizes allowing it to be easily combined with the laser diffraction derived measurements. G2011 is a fine-grained tephra with all grains in the samples <2000 μm; therefore the samples were not sieved. The cone and quartering technique was used to subsample the tephra to be measured in the grain-size analyser. The sample was passed through a cone so that a representative distribution of grain sizes was subsampled for measurement (Blott *et al.* 2004). Raw outputs were converted from increments in μm to half Φ units for analysis and plotting.

Table 1. Details of samples collected for grain-size analysis at each site.

Site	Location	Tephra	Number of thúfur	Number of crest GSD samples	Number of hollow GSD samples
A	63.61377°N 19.96193°W	H1947	50	0	0
B	63.62294°N 19.98391°W	H1947	43	4	43
C	63.96539°N 17.66521°W	G2011	43	43	43

The results of the ultrasonic bath test (Data S3) indicated that using the ultrasonic bath for a 5-min period prior to analysis did not damage or alter the grain-size distribution significantly (Fig. S1, Table S1) and therefore all samples were run through the ultrasonic bath prior to analysis. Trials to remove soil from the tephras (Data S4, Figs S2, S3, Table S2) confirmed that this method worked and all samples were cleaned of soil prior to analysis.

Statistical techniques were used to analyse the data sets collected on tephra layer thickness and GSD to determine if there is a significant difference between tephra layers preserved in crests and hollows of thúfur. Key grain-size statistics (mean, median, standard deviation, etc.) were obtained using the Excel plugin GRADISTAT (version 9.1; Blott & Pye 2001). Median tephra grain size and thickness of the layer are correlated as a function of the distance from the volcanic vent and distance from axis of fall-out, with thinner tephra layers containing finer grain sizes at a landscape scale (Pyle 2016). As data for both parameters were collected in this study, the relationship was tested to examine if this association holds true when tephra layers are deposited across thúfur.

Results

Layer thickness

Variability of tephra and soil thickness in all sites (A–C) is summarized in Fig. 4. At each site the layer thickness was variable: Site A crests ranged 3–29 mm, hollows 0–64 mm, Site B crests 6–14 mm, hollows 11–33 mm (both H1947) and Site C crests 17–98 mm, hollows 30–141 mm (G2011). The results of the paired *t*-test showed that there was a statistically significant difference in tephra thickness between thúfur crests and the hollows at all sites. At all three sites the tephra layers were thicker in the hollows than in the crests (Fig. 4). Soil thickness had a smaller difference between crests and hollows than the tephra layer thickness, particularly in Sites A and C, with mean and standard deviation values similar in both crests and hollows. Site B has a significant difference in soil thickness between crests and hollows, with a thicker soil layer in the crests. Many crests at Site B had little or no tephra layer present. At Site B, only four thúfur crests contained a measurable layer of H1947; however, overlying soil was measured on every crest where sufficient tephra grains were present to define the surface in 1947. Sites A and C had a measurable tephra layer on all crests and hollows.

Tephra thickness measurements from the control sites compared to measurements from thúfur crests and hollows at Sites A–C are also presented in Fig. 4. Both crest and hollow measurements are largely out of range of the control site thicknesses for H1947, although the crests at Site A are very similar to the control thicknesses. G2011 values largely fall within the control ranges, apart from hollow measurements at Site C, which have a much larger range.

Grain-size distribution patterns

Site A did not have samples collected for grain-size analysis (Table 1). Samples for GSD were collected from each region (Hamragarður and Kálfafell) rather than each site. This streamlined the number of samples analysed for GSD. Tephra layer thickness is measured at every site as this is the primary variable investigated, and is able to be tracked across a landscape more easily than GSD. Variation in GSD gives an indication of the processes taking place to redistribute the tephra layer and therefore selective sampling is sufficient. GSD patterns for Sites B and C are presented.

Site B: H1947 tephra. – The overall mean GSD is displayed in Fig. 5A. The GSD on crests and in hollows follow a similar pattern, with a mode of 0 Φ for both crests and hollows, although crests have a slightly higher proportion of large grains than the hollows. Both have a distribution of grains between −2.5 and 5.5 Φ. The GSD for H1947 tephra was unimodal, with a mode centred around 0 Φ in both crests and hollows. Figure 5B shows boxplots of the distribution of median grain-size values for Site B. These indicate that crests have a larger median grain size than hollows, with hollows having a greater variability in grain size than crests. There was no significant difference in mean grain size between the thúfur crests and hollows (Welch two sampled *t*-test: $t(3.6) = 2.44$, $p = 0.078$). There was also no significant difference in median grain size between thúfur crests and hollows (Kruskal–Wallis test: (46) $p = 0.47$). The grain sizes came from different distributions (two sample Kolmogorov–Smirnov test: $D = 0.66$, $p = 0.046$), indicating that populations may differ in median, variability or the shape of the distribution.

Site C: G2011 tephra. – Site C has a complete set of crest and hollow samples, measured from 43 pairs of thúfur,

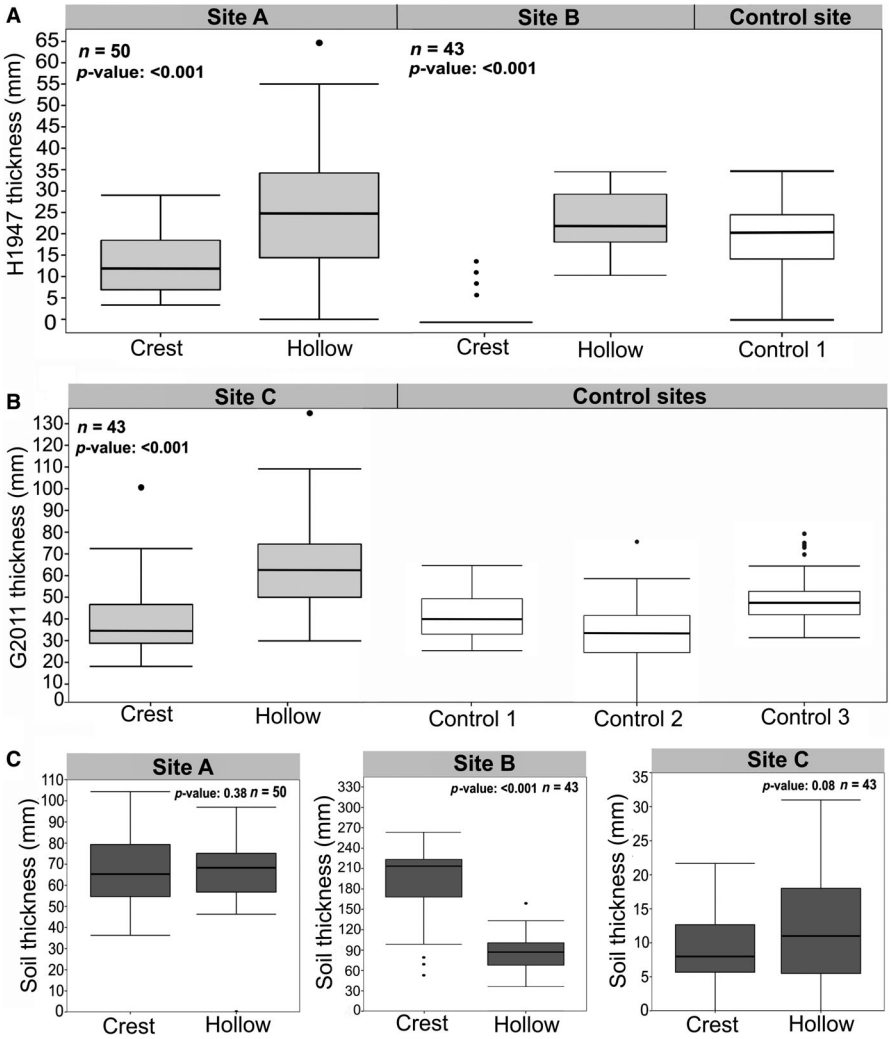

Fig. 4. Comparisons of tephra and soil thickness across thúfur crests and hollows. A. Boxplots of H1947 tephra thickness in Sites A and B indicated in light grey and control measurements from an unthúfured site in white. B. Boxplots of G2011 tephra thickness at Site C indicated in light grey and control measurements from an unthúfured site in white. C. Measurements of soil thickness in crests and hollows from all three sites. *n* denotes the number of measurements collected from each site and the *p*-value the significance of paired *t*-tests.

with the overall mean distribution displayed in Fig. 6A. Crests peak at 2 Φ and hollows at 4 Φ. Crests have a distribution between 0.5 and 7.5 Φ and hollows have a distribution between 1.5 and 7.5 Φ. Boxplots in Fig. 6B show the distribution of median grain-size values for Site C and indicate that crests have a larger median grain size than hollows; however, the crests show a greater variance. There was a significant difference in mean grain size between the thúfur crests and hollows (paired *t*-test: $t(42) = 9.18$, $p < 0.001$). Unlike mean grain size, there was no significant difference between median grain size of crests and hollows (Kruskal–Wallis test: (85), $p = 0.48$). The grain sizes came from different distributions (two sample Kolmogorov–Smirnov test: $D = 0.60$, $p < 0.001$). Thus, the tephra layer is thicker in the hollows, but has a finer grain size than the crests.

Relationship between tephra thickness and grain size

At both Sites B and C median grain size was negatively correlated with tephra layer thickness, for crests and hollows combined (Spearman rank; Site B: $r_s[48] = -0.34$, $p = 0.02$; Site C: $r_s[87] = -0.50$, $p < 0.001$). Therefore, as tephra layer thickness increases, median grain size decreases (Fig. 7). The data were also separated into crests and hollows for each site to examine if this relationship holds when looking at specific locations on the thúfur; Spearman rank Site B: crests $r_s[4] = -0.80$, $p = 0.33$, hollows $r_s[43] = -0.20$, $p = 0.19$. Site C: crests $r_s[43] = -0.48$, $p = <0.001$, hollows $r_s[43] = -0.09$, $p = 0.58$. Results indicate a weak negative correlation for hollows and a moderate to strong correlation for crests at both sites.

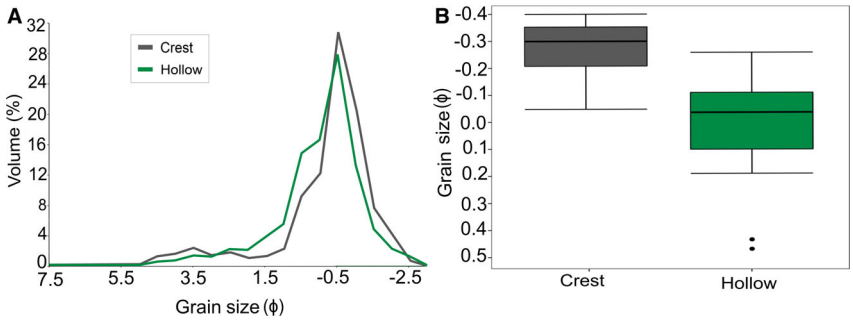

Fig. 5. Hekla 1947 grain-size distribution for crest and hollow locations, Site B. Crest measurements are indicated in grey and hollows in green. A. Overall GSD pattern for H1947 tephra in thúfur crests and hollows at Site B, averaged (mean) from the individual distributions in each crest and hollow measured. B. Boxplots of median grain-size variation of H1947. Smaller particles are denoted by positive values and larger particles by minus phi values.

In summary, tephra thickness varied with location on the thúfur and on average was thicker in hollows than crests. Overlying soil thickness only varied in this way at Site B. In comparison to the control tephra thickness measurements, measurements from thúfur have greater variability in thickness for both H1947 and G2011. Crests contained larger grains than the hollows at both sites, where grain size was measured.

Discussion

Our results show that the characteristics of the tephra layers formed by H1947 and G2011 tephra deposits are influenced by microtopographic variations created by thúfur formations. Across thúfur, hollows develop a thicker tephra layer than crests. GSD show a complex interplay between surface conditions at the time of tephra deposition and the nature of that surface.

Processes controlling tephra thickness and grain-size distribution on thúfur

Our analysis indicates that thicker tephra layers are found in thúfur hollows. For both H1947 and G2011, the tephra layer is consistently ~50% thicker in the hollows than on the crests. The lack of tephra on the crests at Site B in comparison to Site A, 1 km away, could be due to a number of factors. Reworking of the tephra from the crests by Earth surface processes could have occurred as they are more prominent than the hollows. Alternatively, land management practices (such as actively clearing the tephra or grazing livestock) at the time of deposition could have cleared the tephra from the surface. The area is used for sheep and occasional horse grazing today and this is very likely to have been the case at the time of the eruption in 1947, which could have resulted in tephra being cleared so that grazing could continue. The action of grazing in itself could also effectively remove tephra

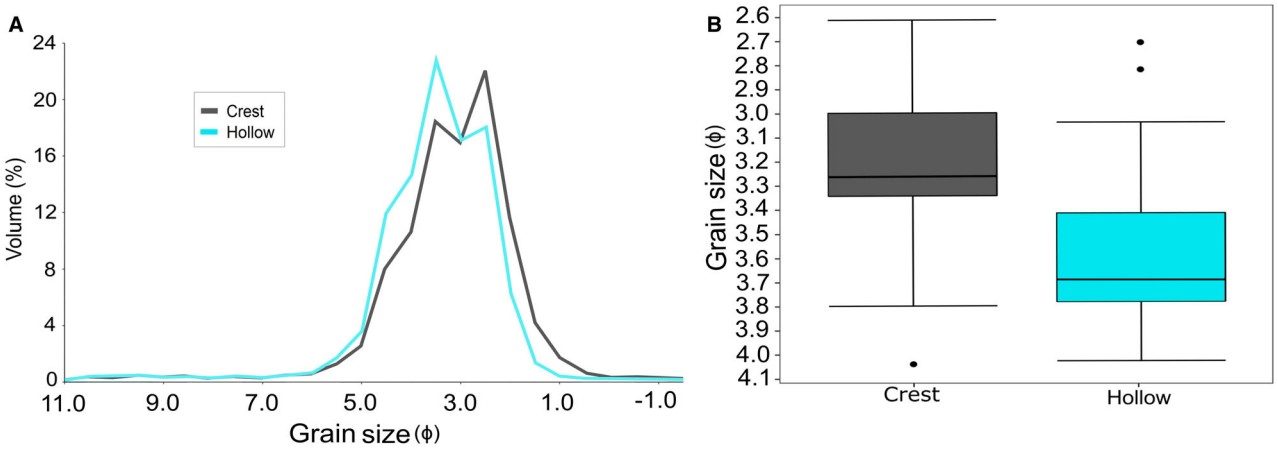

Fig. 6. Grímsvötn 2011 grain-size distribution for crest and hollow locations, Site C. Crest measurements are indicated in grey and hollows in blue. A. Overall GSD pattern for G2011 tephra in thúfur crests and hollows at Site C, averaged (mean) from the individual distributions in each crest and hollow. B. Boxplots of median grain-size variation of G2011. Smaller particles are denoted by positive values and larger particles by minus phi values.

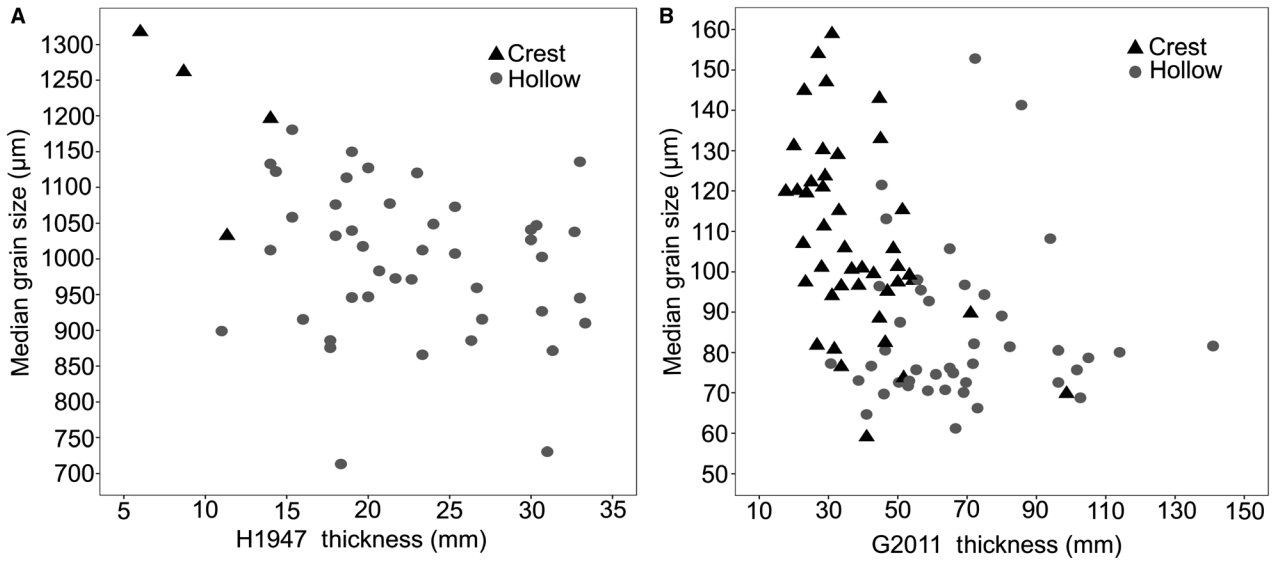

Fig. 7. Scatterplots illustrating the relationship between median grain size of tephra and layer thickness in crests and hollows of thúfur. A. Site B, H1947. B. Site C, G2011.

from thúfur crests preferentially. The thickness of the soil overlaying the H1947 tephra did not exhibit the same pattern of greater accumulation in the hollows (in locations where it was possible to measure this properly). This highlights a fundamental contrast between the gradual, incremental accumulation of aeolian soils across thúfur in particular (and probably variable vegetated microtopography in general), and the episodic deposition of tephra.

At all sites, thickness measurements collected from thúfur show greater variation than the control sites, which have smaller ranges. Therefore, not all measurements from thúfur fall within the range of the controls. This, coupled with the significant difference in tephra thickness between crests and hollows, indicates that the processes operating on thúfur, such as wind, water and movement on slopes, are very effective at redistributing the original fall-out of tephra, compared to a deposit on a surface with few undulations.

Given that the tephra thickness measured in the control sites is more similar to the crests than the hollows, and that the control is considered a reasonable approximation of the original fall-out of both H1947 and G2011 (Cutler *et al*. 2016a, 2018), thúfur crests are more likely to reflect the original fall-out than the hollows. This is not to say that tephra on thúfur crests is exempt from reworking, as is demonstrated by Site B, but overall the formations appear to modify thickness more in the hollows. Similarly, the control measurements are also likely to contain some aeolian reworking as this is difficult to mitigate, but they are still representative as controls given that they were taken from an unthúfured surface. This helps us to separate features that are characteristics of the primary tephra fall-out from those that are acquired due to surface modification, although separating the two is not without its challenges and assumptions.

Crests contain larger grains than hollows, but the significance of this difference varies by site. Mean grain size varies, but medians do not. This indicates the influence of outliers, which skew mean values, but not the medians and is confirmed by KS test results. Although it is difficult to separate the role of the thúfur formations in determining GSD from the other factors, the difference in the grain sizes found in the crests and hollows is important evidence that tephra layers could preserve a record of these formations within their internal structures and GSD. Given these results, we present a number of processes that we believe could be responsible for controlling tephra thickness and grain-size distribution on thúfur.

Surface movements of tephra can occur through the interplay of numerous factors (Arnalds *et al*. 2016). We propose that the differences in preservation observed in this study are the result of slope processes (driven by gravity, water and/or wind movement) and to a lesser extent, vegetation cover. On slopes below 35°, the physical structure of surface vegetation present when tephra is deposited is important in determining the volume of tephra that is incorporated into the stratigraphy at a landscape scale (Antos & Zobel 2006; Cutler *et al*. 2016b; Dugmore *et al*. 2018). Depending upon vegetation height, stem form and packing density, tephra grains are trapped and retained to differing degrees (Shao 2008; Arnalds *et al*. 2016; Dominguez *et al*. 2020). Given the scales at which this operates, the structural variations in the vegetation recorded between crests and hollows surveyed here are too small to drive

any significant difference in relation to the aim of this study.

Thúfur form micro-slopes, often >35°, which is at or above the angle of repose of tephra. Thus, down-slope movement driven by gravity may begin to override the stabilizing effect of surface vegetation. As mean grain size increases, the angle of repose will decrease, as large grains are less cohesive, with grains below 50 μm (4.3 Φ) having greater cohesion and a greater angle of repose (Lu *et al*. 2015; Beakawi Al-Hashemi & Baghabra Al-Amoudi 2018). Thus, one explanation for the thickening of tephra layers in hollows across all sites is that slope angles on thúfur exceed the critical angle of repose. As the slope angles on the thúfur were not measured in detail in this study, but inferred from the vertical and horizontal displacements of crests and hollows, this explanation is speculative and highlights a need to both quantify slope angles on thúfur in greater detail and collect measurements from a variety of slope angles above and below 35°. The potential role of slope in tephra layer formation is summarized in a conceptual model (Fig. 8).

Rainfall and snow-melt increase surface moisture and saturation, which will alter shear stresses operating on the slope and can initiate movement of poorly consolidated surface material, such as tephra (Horton 1933; Major & Yamakoshi 2005). Vegetation cover and the characteristics of soils underlying tephra will affect infiltration and rainfall interception, runoff and erosion rates (Major & Yamakoshi 2005; Cerdà & Doerr 2008; Woods & Balfour 2010; Jones *et al*. 2017). Rainfall simulation studies conducted using freshly fallen tephra deposits by Jones *et al*. (2017) reported that tephra grain movement was dominated by rainsplash detachment of coarse individual grains, with no rill formation or overland flow. They concluded that tephra transport depends on the grain size, with rainsplash the dominant detachment and transport mechanism for coarser (D90: 852.2 μm 0.2 Φ) grained tephra (Jones *et al*. 2017). Finer grained tephra demonstrate more airborne mobilization, pellet formation and increased overland flow due to surface sealing.

Given the evidence that rainsplash detachment of larger grains will be enhanced by steeper slope angles, the patterns in our GSD indicate that water is a key driver of grain movement over the small-scale topography such as thúfur formations. All three sites are similar in terms of past climate data (temperature and precipitation), with both exhibiting cool average temperatures and >1000 mm of rainfall on average most years since records began (Icelandic Meteorological Office 2021). Sites A and B receive greater fluctuations in average rainfall than Site C, but overall all three sites received a substantial volume of rainfall over the year(s) post deposition of the respective tephra. Thus, it is likely that the precipitation coupled with the thúfur formations on each site contributed to the GSD measured and the changing morphology and thickness of the tephra layer.

Freshly deposited tephra is also vulnerable to reworking via wind. Dominguez *et al*. (2020) identified a size range for wind remobilization based on field observations and airborne and ground material samples; 0.4–500 μm. However, Del Bello *et al*. (2021) found that the threshold velocity for entrainment via wind (U^*_{th}) for tephra in real world conditions is much lower than the theoretical value, as theoretical calculations assume grains are spherical, which volcanic ash shards are not. The mean and median grain sizes of G2011 tephra at Site C fall within the range identified by Dominguez *et al*. (2020) in both crests and hollows (mean crests: 129.2 μm (3 Φ) and hollows: 99.3 μm (3.3 Φ)). This indicates that the G2011 deposit was more vulnerable than H1947 to remobilization from wind, although hollows have less of this vulnerable size fraction than crests. The interplay of different factors mean that it is the intermediate fractions of the G2011 deposit, rather than the finest (<3.5 Φ), that are most vulnerable to remobilization from wind (Etyemezian *et al*. 2019; Dominguez *et al*. 2020).

H1947 is a much coarser grained tephra and therefore the most likely transport mechanism for much of this tephra via wind is by creep. Thus, while the bulk of H1947 tephra is less susceptible to remobilization by wind than G2011, other processes are operating to produce similar grain-size patterns. The presence of thúfur will increase surface roughness (Essery & Pomeroy 2004; Wever 2012), with crests and hollows having different, potentially significant, levels of exposure to surface windspeeds. However, this has not yet been tested on small-scale changes in surface roughness created by thúfur, which would provide greater insight into the differences. A summary of the main drivers of the variations in the tephra layers is presented in Table 2.

Implications for the interpretation of landscapes using tephra layers

As highlighted above, tephra sedimentology (tephra layer thickness and GSD) can be used as a tool to help interpret palaeo-landscapes and landscape formations. This work has shown that the morphology of preserved tephra layers and the GSD will be altered by small-scale surface features and by a number of processes operating in conjunction with each other on the surface. Thus, in addition to being used as a chronological tool in palaeo-research, interpreting these alterations will provide additional insight into past landscapes.

Slope angle is clearly important for determining tephra layer thickness. Coarser grained tephra such as H1947 will move on shallower slope angles than a fine-grained tephra, as highlighted in Fig. 8. If a fine-grained tephra, such as G2011 is found to exhibit thickening at certain points in the layer, it can be interpreted as being deposited on a steep (above the critical angle of movement) slope of a greater angle than would be required to move a coarse tephra. When examining tephra layers

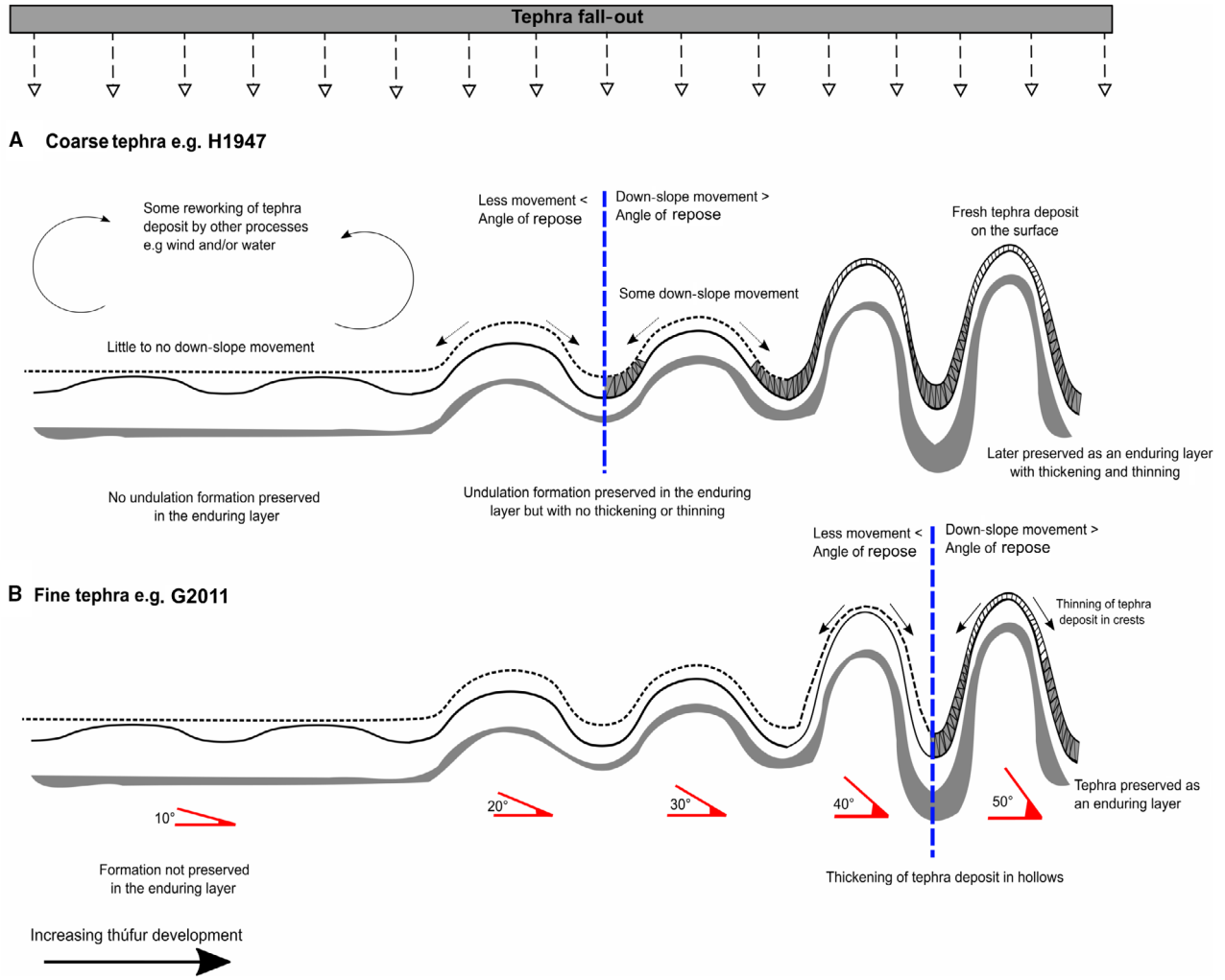

Fig. 8. Conceptual model illustrating the potential movement of a fresh tephra deposit on thúfur formations and the preservation of an enduring tephra layer. We show a range of increasingly well-developed thúfur formations with progressively steeper sides. A. H1947 has a lower critical angle than G2011 and therefore movement is more likely to occur on shallower slopes on the left, with the greatest movement on fully developed thúfur. B. G2011 has a higher angle of repose so more movement is only likely to occur on fully developed thúfur.

across, for example, an archaeological site, finding pockets of thicker tephra can therefore provide information about the angle of slope. A preserved tephra layer with few areas of thickening can be interpreted as being deposited across an area of (relatively) flat land below the critical angle of movement for that tephra, as opposed to a layer that has areas of thickening, thinning and a layer morphology that reflects the ground surface. The presence of small-scale surface features such as thúfur can also be used as a proxy for past climate conditions and/or fluctuations, as the climate must have included freeze–thaw cycles for such features to form and be preserved in the tephra record (Grab 2005; Dugmore *et al.* 2020). Thus, by recording the presence of slope angles above the critical angle of movement, tephra layers can be used to interpret the presence (or absence) of such surface features, which can lead to further interpretations about prevailing climate at the time.

As with slope, tephra size fractions will be moved differently by wind. Both Del Bello *et al.* (2021) and Dominguez *et al.* (2020) concluded that fractions between 50 and 500 μm were most vulnerable to reworking by wind. Some reworking will occur below 50 μm, but very small particles are more cohesive, reducing their mobility (Del Bello *et al.* 2021). The proportion of the H1947 layer <50 μm was 3% on crests and 1% in hollows. In contrast, the figures for G2011 were 24 and 34%, respectively. Finer grained tephras will have a larger portion of grain sizes that are susceptible to aeolian reworking. For very fine grained tephras this will be the intermediate size fraction of the overall GSD, whereas for coarser grained tephras it will be the very smallest fraction or none at all. This is an important consideration when interpreting tephra layers in a landscape, as the preserved layer will partly be the result of reworking, particularly for finer tephras. As we have

Table 2. Summary of the main drivers thought to determine variations in tephra layers on thúfur formations.

Driver	Site A H1947	Site B H1947	Site C G2011	Evidence	Literature
Wind	Undetermined from thickness measurements only	Yes, predominantly creep	Yes, predominantly suspension and saltation	Vulnerable grain-size fraction in both tephras	Dominguez *et al*. (2020); Del Bello *et al*. (2021)
Water	Yes	Yes	Yes	Vulnerable grain-size fraction in both tephras and thickening in hollows	Jones *et al*. (2017)
Vegetation	No	No	No	No significant difference in vegetation structure between crests and hollows	No literature of this occurring on small-scale formations
Slope angle	Yes	Yes	Yes	Thickening in the hollows	Shorts & Feitosa (2018); Dominguez *et al*. (2020)

demonstrated, wind, combined with slope redistributing GSD (crests containing larger particles than hollows), creates a tephra layer with distinctive characteristics that reflect these processes.

Thus, when interpreting the GSD and thickness of a tephra layer, the nature of that tephra layer will to some extent reflect the landscape that it was deposited onto. There are a number of processes occurring at once and it can be challenging to separate out a single environmental signal from a tephra layer. However, by considering the pattern of thickness and GSD changes measured, novel insights (mostly unavailable from other proxies) can be gained. This highlights the utility of tephra layers in palaeoenvironmental research beyond chronology and dating but as a useful tool aiding environmental reconstruction.

Implications for volcanological reconstruction

At a landscape scale, median tephra grain size and thickness of the tephra layer are partly a function of both the distance from the volcanic vent and axis of fall-out (Pyle 2016). In general, thicker tephra layers with larger grain sizes are located close to the vent, thinning and reducing in grain size as one moves further from the volcanic vent (Pyle 1989; Gudnason *et al*. 2018). This pattern is not observed here (Fig. 7) as for both the H1947 and G2011 tephras, thicker layers contain smaller grains, with these thicker layers present in hollows. This is an issue of scale, as the overall pattern will be maintained on the scale of fall-out, but the variation in individual measurements is at a scale of centimetres rather than metres or kilometres. As larger grains were measured in the crests, which have thinner tephra layers, this relationship is not surprising in the context of this study. However, this finding has important implications in terms of volcanological reconstruction.

If we were to reconstruct the eruptions of H1947 and G2011 using the thickness and GSD measurements from this study, the resulting values would be different to those presented in published work. For example, thickness measurements taken by Thorarinsson (1956) to reconstruct the fall-out from H1947 show that Sites A and B are within the 1-cm isopach (Fig. 2). Taking the median thickness measurements from both sites, all apart from crest measurements at Site B show a thickening of tephra, in some cases more than twice as thick (A: crests – 1.1 cm, hollows – 2.5 cm, B: crests – 0 cm, hollows – 2.4 cm). This reinforces the idea that crest values are more representative of the original fall-out than hollows, as discussed above. Sites measured by Cutler *et al*. (2018) to identify how the H1947 layer had been altered since Thorarinsson's original work also showed that in some areas the tephra had increased in thickness. Given the distance from the vent, the grain sizes measured at both Sites A and B are as expected (Pyle 1989). However, the relationship between layer thickness and grain size on the crests is not what would be expected, so sampling from crests only would alter the volcanological reconstruction of the H1947 eruption.

At Site C, the GSD shows a similar pattern to the H1947 sites, with crests containing larger grains than hollows. Whilst the size of the grains is not surprising given the transport distance from the vent, as with the H1947 sites sampling from only crests or hollows would give a skewed GSD, unrepresentative of the original deposit. A detailed isopach map of the G2011 fall-out has not yet been produced, apart from the 1-cm isopach produced by Thordarson & Höskuldsson (2014). More than 1 cm of tephra could therefore have been deposited at Site C and our thickness values suggest this. However, as tephra can become thickened in hollows, thickness from hollows (6.2 cm) is likely to be an exaggeration of the thickness of the original deposit, which may lie closer to the thickness found in the crests (3.5 cm).

Measurements used for volcanological reconstruction are usually collected in a systematic way, often from transects along the axis of fall-out (Bonadonna &

Houghton 2005; Cutler *et al*. 2020). Our measurements were not collected in this way or for this purpose. However, our results highlight that sampling strategy will influence the interpretation of sedimentological records in areas of microtopographic variation, like thúfur fields. Strategic and thorough sampling is therefore desirable, but in palaeo-research it is often not possible to sample as intensively as we have here, for example reconstructions are often conducted from a limited number of cores. Instead, studies should attempt to capture the uncertainty attached to any interpretations made from tephra layers, where possible. In the case of volcanological reconstructions, researchers may consider undertaking a set of calculations using an assumed maximum and minimum range of layer thicknesses, centred on the actual measured thickness of a tephra layer taken from a core. This should then provide a reconstruction that takes into account the alterations that can occur to tephra layers post deposition.

Overall, the findings of this study have clear implications for the interpretation of tephra layers. Alterations that tephra deposits undergo as they are preserved in the stratigraphy can clearly be used to infer environmental processes. We have presented evidence that the presence of thúfur on the surface at the time of tephra deposition is preserved in buried tephra layers. This ability to infer the presence or absence of thúfur has implications in establishing palaeoenvironmental conditions, as freeze–thaw cycles must have existed for thúfur to form, and the soil must have contained enough moisture for this to happen.

Conclusions

There is a thickening of all tephra layers in the hollows of thúfur, regardless of tephra type, and the morphology of the layer follows the shape of the feature. The tephra layers were coarser on the crests. This study has shown that features such as thúfur do indeed drive variations in tephra layer preservation. Differences in thickness are primarily driven by the shape of the formations and the critical slope angle for movement of the tephra.

The G2011 tephra layer at Site C shows a statistically significant difference in grain size, with crests having a larger mean and median grain size than hollows. The H1947 tephra follows a similar pattern, with larger grains in the crests than hollows. As the G2011 and H1947 tephras differ in mean grain size, it is likely that different drivers are relatively more or less important depending on the tephra. But small topographic variations on the land surface result in similar patterns of variation in grain-size distribution, regardless of the mean grain size.

These findings show that variations in the thickness and grain-size distribution of recent tephra layers may be influenced by small-scale topographic variation. Given that this difference is visible in recent layers, we propose that this should also be preserved in older tephra layers, and similar variations may give an indication of land surface features at the time of tephra deposition. Thus, this study adds to a growing body of work that highlights the potential of tephra layer morphology and internal structures as indicators of palaeolandscape conditions, as well as tephra layers' utility as high-quality chrono-lithostratigraphical marker horizons. In addition, it provides important context for the appropriate sampling of tephra layers to infer volcanological processes.

Acknowledgements. – Financial support for this work was provided by NERC Doctoral Training Partnership Ph.D. studentship NE/L002558/1 to Polly I. J. Thompson. We are very grateful to the landowners in Iceland who allowed the fieldwork to take place. Many thanks to our field assistants in August 2019: Martin Dugmore and Connor Morrison. Dr Gavin Sim was most helpful and provided valuable guidance with lab work and particle size analysis of tephra samples. Authors have no conflicts of interest. We are grateful to the reviewers for their comments on the initial manuscript.

Author contributions. – The study was conceived and designed by PIJT, AJD and AJN. Fieldwork and data collection was carried out in 2019 by PIJT, AJD and AJN. Fieldwork to collect control data sets used was carried out by AJD, RTS, NAC and PIJT in 2014/2015. All laboratory work, particle size analysis and statistical analysis was conducted by PIJT. The initial draft of the manuscript was written by PIJT, with subsequent comments and edits made by all other co-authors.

Data availability statement. – All data used in this manuscript are freely available on the University of Edinburgh DataShare facility, which can be accessed via: https://doi.org/10.7488/ds/3104.

References

Antos, J. A. & Zobel, D. B. 2006: Plant responses in forests of the tephra-fall zone. *In* Dale, V. H., Swanson, F. J. & Crisafulli, C. M. (eds.): *Ecological Responses to the 1980 Eruption of Mount St. Helens*, 47–58. Springer, New York.

Arnalds, A. 2005: Approaches to landcare – a century of soil conservation in Iceland. *Land Degradation and Development 16*, 113–125.

Arnalds, O. 2000: The Icelandic Rofabard soil erosion features. *Earth Surface Processes and Landforms 25*, 17–28.

Arnalds, O., Dagsson-Waldhauserova, P. & Olafsson, H. 2016: The Icelandic volcanic aeolian environment: processes and impacts – a review. *Aeolian Research 20*, 176–195.

Beakawi Al-Hashemi, H. M. & Baghabra Al-Amoudi, O. S. 2018: A review on the angle of repose of granular materials. *Powder Technology 330*, 397–417.

Blong, R., Enright, N. & Grasso, P. 2017: Preservation of thin tephra. *Journal of Applied Volcanology 6*, 10, https://doi.org/10.1186/s13617-017-0059-4.

Blott, S. J. & Pye, K. 2001: Gradistat: a grain size distribution and statistics package for the analysis of unconsolidated sediments. *Earth Surface Processes and Landforms 26*, 1237–1248.

Blott, S. J., Croft, D. J., Pye, K., Saye, S. E. & Wilson, H. E. 2004: Particle size analysis by laser diffraction method using reference particles. *Forensic Geoscience: Principles, Techniques and Applications 232*, 63–73.

Bonadonna, C. & Houghton, B. F. 2005: Total grain-size distribution and volume of tephra-fall deposits. *Bulletin of Volcanology 67*, 441–456.

Cabré, J., Aulinas, M., Rejas, M. & Fernandez-Turiel, J. L. 2016: Volcanic ash leaching as a means of tracing the environmental impact of the 2011 Grímsvötn eruption, Iceland. *Environmental Science and Pollution Research 23*, 14338–14353.

Cerdà, A. & Doerr, S. H. 2008: The effect of ash and needle cover on surface runoff and erosion in the immediate post-fire period. *Catena 74*, 256–263.

Cutler, N. A., Bailey, R. M., Hickson, K. T., Streeter, R. T. & Dugmore, A. J. 2016a: Vegetation structure influences the retention of airfall tephra in a sub-Arctic landscape. *Progress in Physical Geography 40*, 661–675.

Cutler, N. A., Shears, O. M., Streeter, R. T. & Dugmore, A. J. 2016b: Impact of small-scale vegetation structure on tephra layer preservation. *Scientific Reports 6*, 37260, https://doi.org/10.1038/srep37260.

Cutler, N., Streeter, R., Engwell, S., Bolton, M., Jensen, B. & Dugmore, A. 2020: How reliable are tephra layers as records of past eruptions? A calibration exercise. *Journal of Volcanology and Geothermal Research*, 106883, https://doi.org/10.1016/j.jvolgeores.2020.106883.

Cutler, N. A., Streeter, R. T., Marple, J., Shotter, L. R., Yeoh, J. S. & Dugmore, A. J. 2018: Tephra transformations: variable preservation of tephra layers from two well-studied eruptions. *Bulletin of Volcanology 80*, 77–92.

Del Bello, E., Taddeucci, J., Merrison, J. P., Rasmussen, K. R., Andronico, D., Ricci, T., Scarlato, P. & Iversen, J. J. 2021: Field-based measurements of volcanic ash resuspension by wind. *Earth and Planetary Science Letters 554*, 116684, https://doi.org/10.1016/j.epsl.2020.116684.

Dominguez, L., Bonadonna, C., Forte, P., Jarvis, P. A., Cioni, R., Mingari, L., Bran, D. & Panebianco, J. E. 2020: Aeolian remobilisation of the 2011-Cordón Caulle tephra-fallout deposit: example of an important process in the life cycle of volcanic ash. *Frontiers in Earth Science 7*, 343, https://doi.org/10.3389/feart.2019.00343.

Dugmore, A. J. & Newton, A. J. 2012: Isochrons and beyond: maximising the use of tephrochronology in geomorphology. *Jökull 62*, 39–52.

Dugmore, A., Streeter, R. & Cutler, N. 2018: The role of vegetation cover and slope angle in tephra layer preservation and implications for Quaternary tephrostratigraphy. *Palaeogeography, Palaeoclimatology, Palaeoecology 489*, 105–116.

Dugmore, A. J., Thompson, P. I., Streeter, R. T., Cutler, N. A., Newton, A. J. & Kirkbride, M. P. 2020: The interpretative value of transformed tephra sequences. *Journal of Quaternary Science 35*, 23–38.

Engwell, S. L., Sparks, R. S. & Aspinall, W. P. 2013: Quantifying uncertainties in the measurement of tephra fall thickness. *Journal of Applied Volcanology 2*, 5, https://doi.org/10.1186/2191-5040-2-5.

Essery, R. & Pomeroy, J. 2004: Vegetation and topographic control of wind-blown snow distributions in distributed and aggregated simulations for an arctic tundra basin. *Journal of Hydrometeorology 5*, 735–744.

Etyemezian, V., Gillies, J. A., Mastin, L. G., Crawford, A., Hasson, R., Van Eaton, A. R. & Nikolich, G. 2019: Laboratory experiments of volcanic ash resuspension by wind. *Journal of Geophysical Research: Atmospheres 124*, 9534–9560.

Grab, S. 2005: Aspects of the geomorphology, genesis and environmental significance of earth hummocks (thúfur, pounus): miniature cryogenic mounds. *Progress in Physical Geography 29*, 139–155.

Guðmundsson, M. T., Höskuldsson, Á., Larsen, G., Thordarson, T., Óladóttir, B. A., Oddsson, B., Gudnason, J., Högnadottir, T., Stevenson, J. A., Houghton, B. F. & Sigudardotttir, G. M. 2012: The May 2011 eruption of Grímsvötn. *Geophysical Research Abstracts 14*, 12119.

Gudnason, J., Thordarson, T., Houghton, B. F. & Larsen, G. 2018: The 1845 Hekla eruption: grain-size characteristics of a tephra layer. *Journal of Volcanology and Geothermal Research 350*, 33–46.

Horton, R. E. 1933: The role of infiltration in the hydrological cycle. *Eos, Transactions American Geophysical UnionEos, Transactions American Geophysical Union 14*, 446–460.

Horwell, C. J., Baxter, P. J., Hillman, S. E., Calkins, J. A., Damby, D. E., Delmelle, P., Donaldson, K., Dunster, C., Fubini, B., Kelly, F. J., Le Blond, J. S., Livi, K. J. T., Murphy, F., Nattrass, C., Sweeney, S., Tetley, T. D., Thordarson, T. & Tomatis, M. 2013: Physicochemical and toxicological profiling of ash from the 2010 and 2011 eruptions of Eyjafjallajökull and Grímsvötn volcanoes, Iceland using a rapid respiratory hazard assessment protocol. *Environmental Research 127*, 63–73.

Icelandic Meteorological Office. 2021: *Monthly Averages of Manned Meteorological Stations*. Available at: https://www.vedur.is/vedur/vedurfar/manadayfirlit (accessed 09.07.2021).

Jones, R., Thomas, R. E., Peakall, J. & Manville, V. 2017: Geomorphology rainfall-runoff properties of tephra: simulated effects of grain-size and antecedent rainfall. *Geomorphology 282*, 39–51.

Liu, E. J., Cashman, K. V., Beckett, F. M., Witham, C. S., Leadbetter, S. J., Hort, M. C. & Guðmundsson, S. 2014: Ash mists and brown snow: remobilization of volcanic ash from recent Icelandic eruptions. *Journal of Geophysical Research: Atmospheres 119*, 9463–9480.

Lowe, D. J. 2011: Tephrochronology and its application: a review. *Quaternary Geochronology 6*, 107–153.

Lu, H., Guo, X., Liu, Y. & Gong, X. 2015: Effect of particle size on flow mode and flow characteristics of pulverized coal. *KONA Powder and Particle Journal 32*, 2015002, https://doi.org/10.14356/kona.2015002.

Major, J. J. & Yamakoshi, T. 2005: Decadal-scale change of infiltration characteristics of a tephra-mantled hillslope at Mount St Helens, Washington. *Hydrological Processes 19*, 3621–3630.

Matheus, P., Begét, J., Mason, O. & Gelvin-Reymiller, C. 2003: Late Pliocene to late Pleistocene environments preserved at the Palisades Site, central Yukon River, Alaska. *Quaternary Research 60*, 33–43.

NCAP (National Collection of Aerial Photography). 2021: Hamragarðar, Iceland. *Aerial photography flown by the Royal Air Force and US Air Force from 1940-1945*. Available at: https://ncap.org.uk/frame/24-1-77-38-36?pos=4264 (accessed 22.07.2021).

Pintaldi, E., D'Amico, M. E., Siniscalco, C., Cremonese, E., Celi, L., Filippa, G., Prati, M. & Freppaz, M. 2016: Hummocks affect soil properties and soil-vegetation relationships in a subalpine grassland (North-Western Italian Alps). *Catena 145*, 214–226.

Pyle, D. M. 1989: The thickness, volume and grainsize of tephra fall deposits. *Bulletin of Volcanology 51*, 1–15.

Pyle, D. M. 2016: Field observations of tephra fallout deposits. *In* Mackie, S., Cashman, K., Ricketts, H., Rust, A. & Watson, M. (eds.): *Volcanic Ash: Hazard Observation*, 25–37. Elsevier, Amsterdam.

R Core Team. 2019: R: A language and environment for statistical computing. R Foundation for Statistical Computing, Vienna, Austria. https://www.R-project.org/.

Rea, H. A., Swindles, G. T. & Roe, H. M. 2012: The Hekla 1947 tephra in the north of Ireland: regional distribution, concentration and geochemistry. *Journal of Quaternary Science 27*, 425–431.

Sanborn, P. T., Smith, C. S., Froese, D. G., Zazula, G. D. & Westgate, J. A. 2006: Full-glacial paleosols in perennially frozen loess sequences, Klondike goldfields, Yukon Territory, Canada. *Quaternary Research 66*, 147–157.

Shao, Y. 2008: *Physics and Modelling of Wind Erosion. Atmospheric and Oceanographic Sciences*, 447 pp. Springer, Amsterdam.

Shorts, D. C. & Feitosa, K. 2018: Experimental measurement of the angle of repose of a pile of soft frictionless grains. *Granular Matter 20*, 2, https://doi.org/10.1007/s10035-017-0774-x.

Stevenson, J. A., Loughlin, S. C., Font, A., Fuller, G. W., MacLeod, A., Oliver, I. W., Jackson, B., Horwell, C. J., Thordarson, T. & Dawson, I. 2013: UK monitoring and deposition of tephra from the May 2011 eruption of Grímsvötn, Iceland. *Journal of Applied Volcanology 2*, 3, https://doi.org/10.1186/2191-5040-2-3.

Streeter, R. T. & Dugmore, A. J. 2013: Reconstructing late-Holocene environmental change in Iceland using high-resolution tephrochronology. *Holocene 23*, 197–207.

Streeter, R. & Dugmore, A. 2014: Late-Holocene land surface change in a coupled social-ecological system, southern Iceland: a cross-scale tephrochronology approach. *Quaternary Science Reviews 86*, 99–114.

Thorarinsson, S. 1944: Tefrokronologiska studier på Island. *Geografiska Annaler 26*, 1–217.

Thorarinsson, S. 1956: The eruption of Mt. Hekla 1947–1948. *Bulletin Volcanologique 10*, 157–168.

Thordarson, T. & Höskuldsson, Á. 2014: *Iceland: Classic Geology in Europe*, 224 pp. Dunedin, Edinburgh.

Thordarson, T. & Larsen, G. 2007: Volcanism in Iceland in historical time: volcano types, eruption styles and eruptive history. *Journal of Geodynamics 43*, 118–152.

Van Vliet-Lanoë, B. & Seppälä, M. 2002: Stratigraphy, age and formation of peaty earth hummocks (pounus), Finnish Lapland. *Holocene 12*, 187–199.

Wever, N. 2012: Quantifying trends in surface roughness and the effect on surface wind speed observations. *Journal of Geophysical Research Atmospheres 117*, D11, https://doi.org/10.1029/2011JD017118.

Woods, S. W. & Balfour, V. N. 2010: The effects of soil texture and ash thickness on the post-fire hydrological response from ash-covered soils. *Journal of Hydrology 393*, 274–286.

Supporting Information

Additional Supporting Information may be found in the online version of this article at http://www.boreas.dk.

Data S1. Tephra thickness control sites.

Data S2. Grain-size distribution sample preparation.

Data S3. Use of ultrasonic bath prior to running samples.

Data S4. Cleaning of samples.

Fig. S1. Plots of GSD of the same sample that have and have not been treated with an ultrasonic bath. Samples that have not been treated with an ultrasonic bath were instead left overnight in a dispersant agent.

Fig. S2. Plots of GSD of the same sample that has been cleaned and not cleaned using an ultrasonic bath.

Fig. S3. Results of method to remove soil contamination from tephra samples. The image shows a sample of G2011 tephra that was split so that half has had the ultrasonic process to remove soils performed (right) and the other has not (left). The left sample has a clear layer of pale grey silt on top of the tephra, whereas this layer is not observed in the sample on the right.

Table S1. Summary statistics of samples treated with the ultrasonic bath (blue) and without (red). Values in μm were converted to phi using the equation $ø = -\log_2(D/D_0)$, where D is the diameter of the grain in mm and D_0 is the reference diameter equal to 1 mm.

Table S2. Summary statistics of samples that have been cleaned using an ultrasonic bath (purple) and samples that have not been cleaned (teal). Values in μm were converted to phi using the equation $ø = -\log_2(D/D_0)$, where D is the diameter of the grain in mm and D_0 is the reference diameter equal to 1 mm.

Table S3. Table summarizing the *p*-values from statistical tests run on samples used to test the cleaning method using an ultrasonic bath.